J Electr Eng Technol Vol. 9, No. 3: 873-881, 2014
http://dx.doi.org/10.5370/JEET.2014.9.3.873

ISSN(Print) 1975-0102
ISSN(Online) 2093-7423

Sensorless Vector Control of Induction Motors for Wind Energy Applications Using MRAS and ASO

Il-Woo Jeong*, Won-Shik Choi and Ki-Hyeon Park†**

Abstract – Speed sensorless modes of operation are becoming standard solution in the area of electric drives. This paper presents flux estimator and speed estimator for the speed sensorless vector control of induction motors. The proposed sensorless methods are based on the model reference adaptive system (MRAS) observer and adaptive speed observer (ASO). The proposed speed estimation algorithm can be employed in the power control of grid connected induction generator for wind power applications. Two proposed schemes are verified through computer simulation PSIM and compared their simulation results.

Keywords: Wind energy, Sensorless vector control, Induction motor, Model reference adaptive system(MRAS), Adaptive speed observer(ASO)

Nomenclature

General:

R	Resistance
L	Inductance
λ	Flux linkage
ω_e	Electrical angular frequency
ω_r	Rotational angular frequency
ω_c	Transition frequency
ω_{rm}	Mechanical angular frequency
ω_{sl}	Slip angular frequency
θ_e	Electrical angle
θ_r	Mechanical angle
T_e	Electrical torque
T_{ae}	Aerodynamic torque
u	Wind speed
U_m	Mean wind speed
$u(t,r,\theta_b)$	Wind field
$u_\psi(t,\theta_b)$	Weighted wind speed
M_b	Blade root moment
$M(U_m)$	Steady state blade root moment
$S_k(f)$	Power spectral density of wind speed
$F_k(f)$	Admittance function
σ	Induction motor leakage coefficient
p	Time derivative
P	Number of pole pairs
K_p	Proportional gain
K_i	Integral gain
k	Proportional constant(>0)
γ	Positive real number

Superscript:

^	Estimated value
*	Reference value
~	Azimuth expansion
s	Stationary reference frame
r	Rotor reference frame
e	Synchronously rotating reference frame

Subscript:

a, b, c	Basic three phase
d, q	Direct axis, quadrature axis
r, s	Rotor, stator
m	Mutual
l	Leakage
eq	Equivalent

† Corresponding Author: Pohang Accelerator Laboratory (PAL), Pohang University of Science and Technology (POSTECH), Korea. (pkh@postehc.ac.kr)
* Graduate school for Wind Energy, Pohang University of Science and Technology (POSTECH), Korea. (jiw88@postehc.ac.kr)
** Graduate school for Wind Energy, Pohang University of Science and Technology (POSTECH), Korea. (whatcc@postech.ac.kr)
Received: September 9, 2013; Accepted: November 28, 2013

1. Introduction

The induction motors are widely used for wind energy conversion systems. The advantages of general induction motors in wind energy system are relatively inexpensive, robust and require low maintenance [1-2]. In addition to using vector control techniques, fast dynamic response and accurate torque control can be possible. For vector control, rotor speed information is essential. Usually, an encoder or a tachometer is used to measure the generator speed. The speed sensors may result in many practical disadvantages. Therefore, by eliminating the speed sensor, reliability of wind turbine drive is improved and cost is reduced.

The various different solutions for sensorless drives were proposed in the past decade. For example, the rotor speed and position can be estimated based on the stator voltage equation of the AC motor [3], reference model of

the AC motor [4], state observer [5], back EMF [6], the Kalman filtering [7], nonlinear control [8], signal injection [9] and fuzzy control [10].

Among the approaches described above, model reference adaptive system (MRAS) and adaptive speed observer (ASO) are attractive due to their design simplicity. The MRAS observer is based on the voltage model and current model. The method to calculate rotor flux linkage using the stator voltage equation is called the voltage model method. The method to calculate rotor flux linkage using rotor voltage equation, where the voltage is zero in the case of the squirrel cage rotor and only the current is the variable, is called the current model method [11]. The ASO method is based on a speed adaptive flux observer using the adaptive control theory. This method uses the state observer which can allocate poles arbitrarily. Therefore, it can be applied to the direct field-oriented control, even in a low speed region [12].

In this paper a variable speed wind turbine system described by induction motor-generator set. The system consists of motor control inverter and back-to-back converter(combination of the generator side and grid side PWM converter). The motor control inverter simulated the blade part of wind turbine system. The rotor wind model obtained from the equivalent wind speed [13], turbulence model [13] and tower shadow effect [14]. Wind speed-blade power coefficient(Cp) data and rpm-torque data obtained from the National Renewable Energy Laboratory (NREL) 5MW reference wind turbine model. The back-to-back converter performed the generator control(including two kinds of sensorerlss control algorithm) and grid connection control.

2. Induction Motor D-Q Model and Vector Control

2.1 Mathematical model of an induction motor

Prior to explain vector control for induction motor, determine the d-q model of the induction motor via mathematical model representing the dynamic characteristics of the motor [15]. The stator and rotor voltage equations in synchronously rotating reference frame can be expressed as (1). The stator and rotor flux linkage equations in synchronously rotating reference frame can be expressed as (2). Fig. 1 shows the equivalent circuit of an induction motor.

$$\begin{aligned} v_{dqs}{}^{e} &= R_s i_{dqs}{}^{e} + \left(d\lambda_{dqs}{}^{e}/dt\right) \mp \omega_e \lambda_{dqs}{}^{e} \\ v_{dqr}{}^{e} &= R_r i_{dqr}{}^{e} + \left(d\lambda_{dqr}{}^{e}/dt\right) \mp (\omega_e - \omega_r)\lambda_{dqr}{}^{e} \end{aligned} \tag{1}$$

$$\begin{aligned} \lambda_{dqs}{}^{e} &= L_{ls} i_{dqs}{}^{e} + L_m \left(i_{dqs}{}^{e} + i_{dqr}{}^{e}\right) = L_s i_{dqs}{}^{e} + L_m i_{dqr}{}^{e} \\ \lambda_{dqr}{}^{e} &= L_{lr} i_{dqr}{}^{e} + L_m \left(i_{dqs}{}^{e} + i_{dqr}{}^{e}\right) = L_r i_{dqr}{}^{e} + L_m i_{dqs}{}^{e} \end{aligned} \tag{2}$$

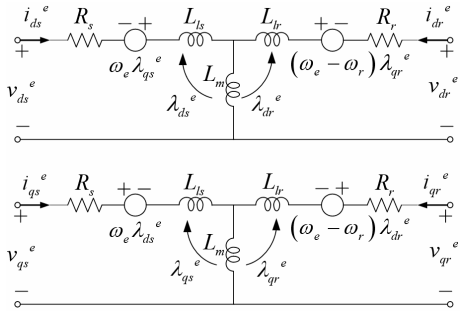

Fig. 1. d-q axes equivalent circuit of an induction motor.

2.2 Vector control of an induction motor

Vector control methods can be classified into two methods as the direct method and the indirect method according to the way of obtaining the flux angle information.

In the direct vector control method [15], the information of rotor flux linkage is obtained by measurement or calculation. All currents decomposed to the flux component current and torque component current based on the flux information. In general, the flux component current is controlled to be constant and the torque component current is controlled instantaneously depending on the reference torque value. The relationship between the d axis stator current and rotor flux linkage can be described as

$$\lambda_{dr}{}^{e} = L_m i_{ds}{}^{e} - \frac{L_r}{R_r} p\lambda_{dr}{}^{e} = \frac{L_m}{1 + p\left(L_r / R_r\right)} i_{ds}{}^{e} \tag{3}$$

The relationship between the q axis current and electrical torque can be described as

$$T_e = \frac{\mathrm{P}}{2}\frac{3}{2}\frac{L_m}{L_r}\lambda_{dr}{}^{e} i_{qs}{}^{e} = \frac{\mathrm{P}}{2}\frac{3}{2}\frac{L_m^{\,2}}{L_r} i_{ds}{}^{e} i_{qs}{}^{e} \tag{4}$$

The reference stator current of d-q axes in synchronously rotating reference frame can be described as

$$\begin{aligned} i_{ds}{}^{e*} &= \left(\lambda_{dr}{}^{e*} / L_m\right) \\ i_{qs}{}^{e*} &= \left(T_e{}^{*} / K_T\right) \ , \ (K_T = \frac{\mathrm{P}}{2}\frac{3}{2}\left(L_m / L_r\right)\lambda_{dr}{}^{e}) \end{aligned} \tag{5}$$

Three-phase stator current reference equations can be described as

$$\begin{aligned} i_{as}{}^{*} &= i_{ds}{}^{s*} \\ i_{bs}{}^{*} &= -(1/2) i_{ds}{}^{s*} + \left(\sqrt{3}/2\right) i_{qs}{}^{s*} \\ i_{cs}{}^{*} &= -(1/2) i_{ds}{}^{s*} - \left(\sqrt{3}/2\right) i_{qs}{}^{s*} \end{aligned} \tag{6}$$

The stator current follow the reference current by the current controller, instantaneous torque control is achieved.

3. Sensorless Control Algorithm

3.1 MRAS for an induction motor

The model reference adaptive system consists of voltage model and current model. In the voltage model [11], the rotor flux linkage is obtained from the stator flux linkage information. And the stator flux linkage information is obtained from the stator voltage equation. For this process, stator voltage and current are needed. By integrating the stator voltage of d-q axes in stationary reference frame, stator flux linkage is obtained as

$$v_{dqs}{}^{s} = R_s i_{dqs}{}^{s} + \left(d\lambda_{dqs}{}^{s} / dt \right) \tag{7}$$

$$\lambda_{dqs}{}^{s} = \int \left(v_{dqs}{}^{s} - R_s i_{dqs}{}^{s} \right) dt \tag{8}$$

The rotor current can be expressed as stator flux linkage and stator current. Substitute the rotor current into the rotor flux linkage of d axis in stationary reference frame.

$$i_{dr}{}^{s} = \left(\lambda_{ds}{}^{s} - L_s i_{ds}{}^{s} \right) / L_m \;\rightarrow\; \lambda_{dr}{}^{s} = L_r i_{dr}{}^{s} + L_m i_{ds}{}^{s} \tag{9}$$

$$\lambda_{dr}{}^{s} = \left(L_r / L_m \right) \left(\lambda_{ds}{}^{s} - \sigma L_s i_{ds}{}^{s} \right), \;\; \left(\sigma = 1 - (L_m{}^{2} / L_s L_r) \right) \tag{10}$$

With the same process, the rotor flux linkage equation of q axis and the electrical angle is obtained as

$$\begin{aligned} &\lambda_{qr}{}^{s} = L_r i_{dr}{}^{s} + L_m i_{qs}{}^{s} = \left(L_r / L_m \right) \left(\lambda_{qs}{}^{s} - \sigma L_s i_{qs}{}^{s} \right) \\ &\theta_e = \tan^{-1} \left(\lambda_{qr}{}^{s} / \lambda_{dr}{}^{s} \right) \end{aligned} \tag{11}$$

The voltage model method is based on obtained the rotor flux by integrating back EMF of induction motor. In the high-speed operation area where the magnitude of back EMF is large enough, the voltage model method shows a good performance.

In the current model [11], the rotor speed and stator current information are obtained from the rotor voltage equation. Finally, the rotor flux linkage is obtained from the rotor speed and stator current information. The rotor flux linkage equation of d-q axes in the rotor reference frame can be calculated based on the rotor flux and stator current in the rotor reference frame. And the stator current of d-q axes in the rotor reference frame can be obtained from coordinate transformation theory.

$$p\lambda_{dqr}{}^{r} = -\left(R_r / L_r \right) \lambda_{dqr}{}^{r} + R_r \left(L_m / L_r \right) i_{dqs}{}^{r} \tag{12}$$

$$\begin{cases} i_{ds}{}^{r} = i_{ds}{}^{s} \cos\theta_r + i_{qs}{}^{s} \sin\theta_r \\ i_{qs}{}^{r} = -i_{ds}{}^{s} \sin\theta_r + i_{qs}{}^{s} \cos\theta_r \end{cases} \tag{13}$$

By integrating (12) and using (13), the rotor flux linkage of d-q axes in the stationary reference frame can be obtained as

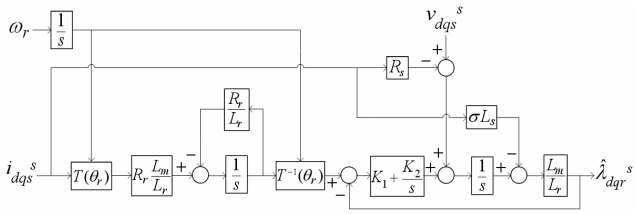

Fig. 2. The combination of voltage model and current model.

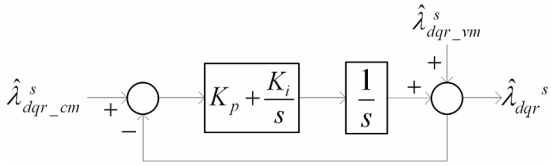

Fig. 3. The simplified block diagram of combination estimator.

$$\begin{cases} \lambda_{dr}{}^{s} = \lambda_{dr}{}^{r} \cos\theta_r - \lambda_{qr}{}^{r} \sin\theta_r \\ \lambda_{qr}{}^{s} = -\lambda_{dr}{}^{r} \sin\theta_r + \lambda_{qr}{}^{r} \cos\theta_r \end{cases} \tag{14}$$

The current model method is based on the flux obtained by using the rotor speed, exact information of rotor resistance and rotor inductance. Thus the speed and position sensorless control, induction machine parameter estimation and real-time parameter tuning are needed. The current model is useful in zero-speed or low-speed operation area because in the high-speed operation area the current model method shows a little unstable performance.

As a result, current model is an advantageous method in low-speed operation area, and voltage model is an advantageous method in high-speed operation area. So the combination of two models has a good performance in wide speed range. The block diagram of combination is shown in Fig. 2 and the simplified block diagram is shown in Fig. 3.

The simplified block diagram consists of estimated rotor flux linkage from the current model, estimated rotor flux linkage from the voltage model and PI controller.

The transfer function of the simplified block diagram of the estimator is expressed as

$$\hat{\lambda}_{dqr}{}^{s} = \frac{s^2}{s^2 + K_p s + K_i} \hat{\lambda}_{dqr\_vm}^{s} + \frac{K_p s + K_i}{s^2 + K_p s + K_i} \hat{\lambda}_{dqr\_cm}^{s} \tag{15}$$

The transfer function consists of the flux linkage from the current model with the low-pass filter and the flux linkage from the voltage model with the high-pass filter. The PI controller gains are described as (16).

$$K_p = \sqrt{2}\omega_c \;,\; K_i = \omega_c{}^{2} \quad (\zeta = 0.707) \tag{16}$$

The estimated rotor speed can be obtained by using the estimated slip angular frequency and estimated electrical

frequency and slip angular frequency.

$$\hat{\omega}_e = \frac{d}{dt}\tan^{-1}\left(\frac{\hat{\lambda}_{dr}{}^s}{\hat{\lambda}_{qr}{}^s}\right) = \frac{\left(\hat{\lambda}_{qr}{}^s\right)'\hat{\lambda}_{dr}{}^s - \left(\hat{\lambda}_{dr}{}^s\right)\hat{\lambda}_{qr}{}^s}{\left(\hat{\lambda}_{dr}{}^s\right)^2 + \left(\hat{\lambda}_{qr}{}^s\right)^2} \quad (17)$$

$$\hat{\omega}_{sl} = \frac{R_r}{\left(\hat{\lambda}_{dr}{}^s\right)^2 + \left(\hat{\lambda}_{qr}{}^s\right)^2}\left\{\frac{L_m}{L_r}\left(\hat{\lambda}_{dr}{}^s i_{qs}{}^s + \hat{\lambda}_{qr}{}^s i_{ds}{}^s\right)\right\} \quad (18)$$

Then the estimated rotor angular frequency ($\hat{\omega}_r$) can be obtained from the difference between estimated electrical frequency and estimated slip angular frequency.

$$\begin{aligned}\hat{\omega}_r &= \hat{\omega}_e - \hat{\omega}_{sl} \\ &= \frac{\left(\hat{\lambda}_{qr}{}^s\right)'\hat{\lambda}_{dr}{}^s - \left(\hat{\lambda}_{dr}{}^s\right)\hat{\lambda}_{qr}{}^s}{\left(\hat{\lambda}_{dr}{}^s\right)^2 + \left(\hat{\lambda}_{qr}{}^s\right)^2} - \frac{R_r L_m}{L_r}\frac{\hat{\lambda}_{dr}{}^s i_{qs}{}^s + \hat{\lambda}_{qr}{}^s i_{ds}{}^s}{\left(\hat{\lambda}_{dr}{}^s\right)^2 + \left(\hat{\lambda}_{qr}{}^s\right)^2}\end{aligned} \quad (19)$$

3.2 ASO for an induction motor

In the adaptive speed observer method [12], the rotor speed information is based on state equation of induction machine and state observer. An induction machine can be expressed as following state equations in the stationary reference frame as

$$\frac{d}{dt}\begin{bmatrix}\mathbf{i}_s \\ \boldsymbol{\lambda}_r\end{bmatrix} = \begin{bmatrix}\mathrm{A}_{11} & \mathrm{A}_{12} \\ \mathrm{A}_{21} & \mathrm{A}_{22}\end{bmatrix}\begin{bmatrix}\mathbf{i}_s \\ \boldsymbol{\lambda}_s\end{bmatrix} + \begin{bmatrix}\mathbf{B}_1 \\ 0\end{bmatrix}\mathbf{V}_s = \mathbf{AX} + \mathbf{BV}_s \quad (20)$$

$$\mathbf{i}_s = \mathbf{CX} \quad (21)$$

where

$$\mathbf{X} = \begin{bmatrix} i_{ds}{}^s & i_{qs}{}^s & \lambda_{dr}{}^s & \lambda_{qr}{}^s \end{bmatrix}^T$$

$$\mathbf{i}_s = \begin{bmatrix} i_{ds}{}^s & i_{qs}{}^s \end{bmatrix}^T,\ \boldsymbol{\lambda}_r = \begin{bmatrix} \lambda_{ds}{}^s & \lambda_{qr}{}^s \end{bmatrix}^T$$

$$\mathrm{A}_{11} = -\left\{R_s/\sigma L_s + (1-\sigma)/\sigma\tau_r\right\}\mathrm{I} = a_{r11}\mathrm{I},$$

$$\mathrm{A}_{12} = L_m/\sigma L_s L_r\left\{(1/\tau_r)\mathrm{I} - \omega_r\mathrm{J}\right\} = a_{r12}\mathrm{I} + a_{i12}\mathrm{J},$$

$$\mathrm{A}_{21} = (L_m/\tau_r)\mathrm{I} = a_{r21}\mathrm{I},\ \mathrm{A}_{22} = -(1/\tau_r)\mathrm{I} + \omega_r\mathrm{J} = a_{r22}\mathrm{I} + a_{i22}\mathrm{J},$$

$$\mathrm{B}_1 = (1/\sigma L_s)\mathrm{I} = b_1\mathrm{I},\ \mathrm{C} = \begin{bmatrix}\mathrm{I} & 0\end{bmatrix},\ \mathrm{I} = \begin{bmatrix}1 & 0 \\ 0 & 1\end{bmatrix},\ \mathrm{J} = \begin{bmatrix}0 & -1 \\ 1 & 0\end{bmatrix}$$

The state observer that estimate the stator current and the rotor flux linkage together can be expressed as (22). From the state equations of induction machine and state observer, the error of stator current and rotor flux linkage is can be calculated as (23).

$$\frac{d}{dt}\hat{\mathbf{X}} = \hat{\mathbf{A}}\hat{\mathbf{X}} + \mathbf{BV}_s + \mathbf{G}(\hat{\mathbf{i}}_s - \mathbf{i}_s) \quad (22)$$

$$\frac{d}{dt}\mathbf{e} = (\mathbf{A} - \mathbf{GC})\mathbf{e} - \Delta\mathbf{A}\hat{\mathbf{X}} \quad (23)$$

where

$$\mathbf{e} = \mathbf{X} - \hat{\mathbf{X}},\ \Delta\mathbf{A} = \hat{\mathbf{A}} - \mathbf{A} = \begin{bmatrix}0 & -\Delta\omega_r\mathbf{J}/c \\ 0 & \Delta\omega_r\mathbf{J}\end{bmatrix}$$

$$\mathbf{V}_S = \begin{bmatrix} V_{ds}{}^s & V_{qs}{}^s \end{bmatrix}^T,\ \mathbf{C} = \begin{bmatrix}\mathbf{I} & 0\end{bmatrix},\ C = \frac{\sigma L_s L_r}{L_m},\ \Delta\omega_r = \hat{\omega}_r - \omega_r$$

When Lyapunov function defines as (24), the time differentiation of Lyapunov function (V) depending on time and it can be expressed as (25). The Adaptive Law of speed estimation can be expressed as (26) by nullifying the sum of second and third terms on the right-hand side.

$$\mathbf{V} = \mathbf{e}^T\mathbf{e} + \left(\hat{\omega}_r - \omega_r\right)^2/\gamma \quad (24)$$

$$\begin{aligned}\frac{d}{dt}\mathbf{V} = \mathbf{e}^T&\left\{(\mathbf{A}+\mathbf{GC})^T + (\mathbf{A}+\mathbf{GC})\right\}\mathbf{e} \\ &- 2\Delta\omega_r\left(e_{ids}\hat{\lambda}_{qr}{}^s - e_{iqs}\hat{\lambda}_{dr}{}^s\right)/c + 2\Delta\omega_r\frac{d}{dt}\frac{\hat{\omega}_r}{\gamma}\end{aligned} \quad (25)$$

$$\frac{d}{dt}\hat{\omega}_r = \frac{\gamma\left(e_{ids}\hat{\lambda}_{qr}{}^s - e_{iqs}\hat{\lambda}_{dr}{}^s\right)}{c} \quad (26)$$

where $e_{ids} = i_{ds}{}^s - \hat{i}_{ds}{}^s$, $e_{iqs} = i_{qs}{}^s - \hat{i}_{qs}{}^s$.

Because the speed of induction machine changes very fast, substantially PI controller used to increase convergence speed of the speed estimation (27). General block diagram of speed adaptive observer is shown in Fig.4.

$$\begin{aligned}\hat{\omega}_r &= K_p\left(e_{ids}\hat{\lambda}_{qr}{}^s - e_{iqs}\hat{\lambda}_{dr}{}^s\right) \\ &\quad + K_i\int_0^t\left(e_{ids}\hat{\lambda}_{qr}{}^s - e_{iqs}\hat{\lambda}_{dr}{}^s\right)d\tau\end{aligned} \quad (27)$$

where the observer gain matrix(G) is given as follows:

$$\mathbf{G} = \begin{bmatrix} g_1 & g_2 & g_3 & g_4 \\ -g_2 & g_1 & -g_4 & g_3 \end{bmatrix}^T$$

$$g_1 = (k-1)(a_{r11} + a_{r22}),\ g_2 = (k-1)a_{i22}$$

$$g_3 = (k^2-1)(ca_{r11} + a_{r21}) - c(k-1)(a_{r11} + a_{r22})$$

$$g_4 = -c(k-1)a_{i22}$$

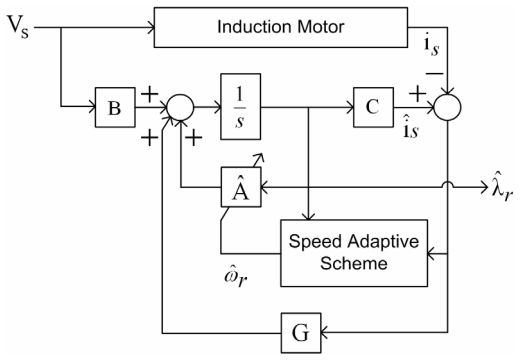

Fig. 4. General block diagram of adaptive speed observer.

4. Equivalent Wind Model

4.1 Rotor model

The rotor model is derived from the torque generated from the turbulence in the rotor plane. Parameters of wind turbine in the rotor plane are shown in Fig. 5.

The aerodynamic torque is given as the sum of the blade root moments [13].

$$T_{ae}(t) = \sum_{b=1}^{3} M_b(t) \tag{28}$$

$$M_b(t) = M(U_m) + \int_{r_0}^{R} \psi(r)(u(t,r,\theta_b)) - U_m)dr \tag{29}$$

$$\begin{aligned} T_{ae}(t) &= 3M(U_m) + \sum_{b=1}^{3}\int_{r_0}^{R} \psi(r)(u(t,r,\theta_b) - U_m)dr \\ &= 3M(U_m) + \sum_{b=1}^{3}\int_{r_0}^{R} \psi(r)(u_{eq}(t) - U_m)dr \end{aligned} \tag{30}$$

The aerodynamic torque equation can be summarized as follow equivalent wind speed equation.

$$u_{eq}(t) = \frac{1}{3}\sum_{b=1}^{3} u_{\psi}(t,\theta_b) \tag{31}$$

$$u_{\psi}(t,\theta_b) = \frac{\int_{r_0}^{R} \psi(r)u(t,r,\theta_b)dr}{\int_{r_0}^{R} \psi(r)dr} = \sum_{k=-\infty}^{\infty} \tilde{u}_{\psi,k}(t)e^{\mathrm{j}k\theta_b} \tag{32}$$

Substituting the weighted wind speed ($u_{\psi}(t,\theta_b)$), the equivalent wind speed can be approximated by the sum of the 0th and 3rd harmonic components.

$$\begin{aligned} u_{eq}(t) = &\sum_{k=-\infty}^{\infty} \tilde{u}_{\psi,\,3k}(t)e^{\mathrm{j}3k\theta_{WTR}} \approx \tilde{u}_{\psi,0}(t) \\ &+ 2\,\mathrm{Re}\{\tilde{u}_{\psi,3}(t)\}\cos(3\theta_{WTR}) \\ &+ 2\,\mathrm{Im}\{\tilde{u}_{\psi,3}(t)\}\sin(3\theta_{WTR}) \end{aligned} \tag{33}$$

3rd azimuth expansion coefficient ($\tilde{u}_{\psi,\,3k}(t)$) is determined by the turbulence model and tower shadow effect.

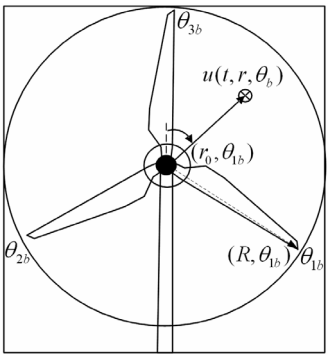

Fig. 5. Parameters of wind turbine in the rotor plane.

4.2 Turbulence model

The turbulence model generates the azimuth expansion coefficients of the turbulence field ($\tilde{u}_{\psi,k,turb}(t)$). The power spectral density (PSD) of $\tilde{u}_{\psi,k,turb}(t)$ can be obtained by multiplying the PSD of the wind speed in a fixed point and admittance function [13].

$$S_{\tilde{u}_{\psi,k}}(f) = F_{\tilde{u}_{\psi,k}}(f) \cdot S_u(f) \tag{34}$$

Using the numerical results by P. Sørensen [16] and W. Langreder [17], the 0th and 3rd harmonic components of equivalent wind speed can be fitted to linear filters [13].

$$\begin{aligned} H_{\psi,0}(s) &\approx \frac{0.99 + 4.79ds}{1 + 7.35ds + 7.68(ds)^2} \\ H_{\psi,3}(s) &\approx \frac{0.0307 + 0.277ds}{1 + 1.77ds + 0.369(ds)^2}, \quad d = \frac{R_b}{V_0} \end{aligned} \tag{35}$$

4.3 Tower shadow effect

Parameters of tower shadow effect are shown in Fig. 6. The wind speed which is affected by tower shadow effect can be represented as [14]

$$u_{tow} = U_m\left(1 - \frac{(D_t/2)^2\left(x^2 - y^2\right)}{\left(x^2 + y^2\right)^2}\right) \tag{36}$$

Considering overhang and diameter of tower of reference generator, x/D which is real distance of blade is

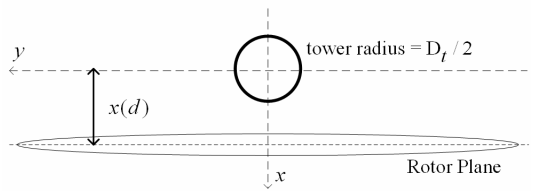

Fig. 6. Parameters of tower shadow effect.

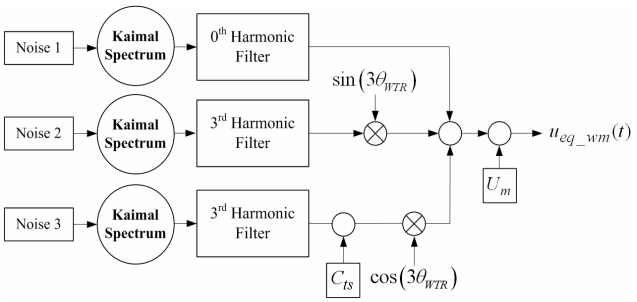

Fig. 7. Overall process for generate equivalent wind model.

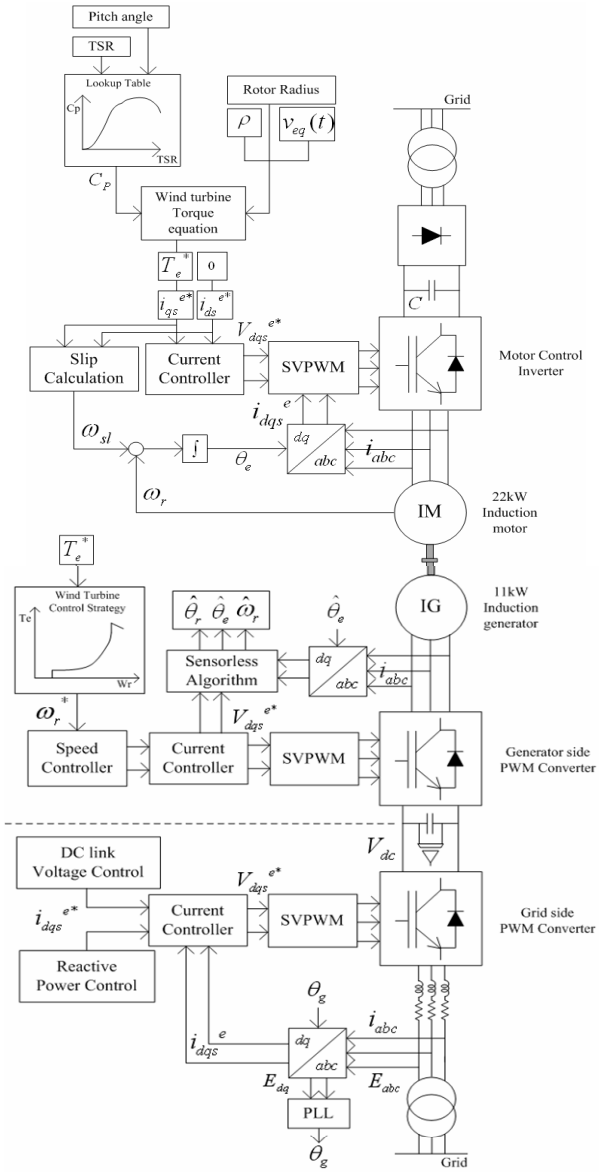

Fig. 8. Overall control scheme

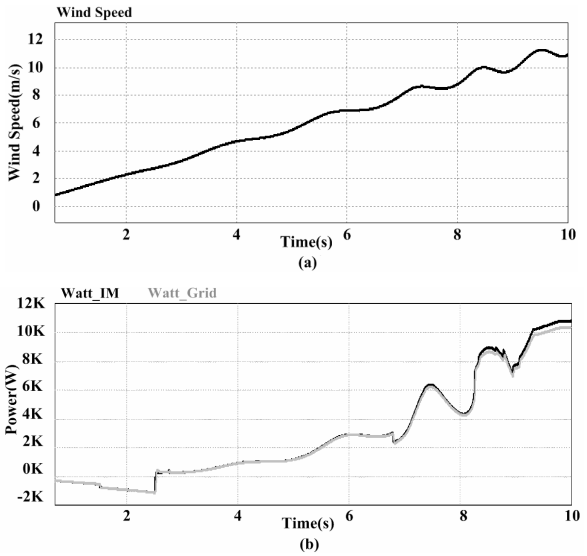

Fig. 9. (a) Equivalent wind speed; (b) Active power from generator(black) and flowing into the grid(gray).

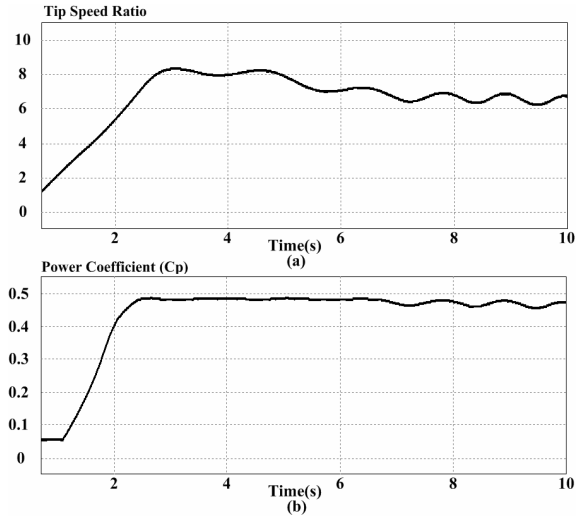

Fig. 10. (a) Power coefficient (Cp). (b) Tip speed ratio.

defined as 1.513. Finally, C_{ts} can be approximated as

$$C_{ts} \approx \frac{u_{tow}}{3} \tag{37}$$

As a result, overall process to generate equivalent wind model ($u_{eq\_wm}(t)$) are shown in Fig. 7.

5. Simulation Results

To demonstrate the performance of sensorless vector control, simulation works in PSIM with Microsoft Visual Studio 2010. The motor and generator set consists of 22kW and 11kW respectively. Parameters of two induction motors are shown in the APPENDIX respectively.

Fig. 8 shows the overall control scheme. The motor control inverter generates the torque reference for motor control using equivalent wind speed and power coefficient. The back to back converter controlled the generator part and grid connection system. The generator side converter carried out generator speed control, current control and two kinds of sensoreless controls. The grid side converter carried out DC link voltage control, reactive/active power control, phase locked loop (PLL) control and satisfied the requirements of gird code.

Fig. 9(a) shows the equivalent wind speed increase from zero to 11.4m/s and includes turbulence model (turbulence intensity is 19.8%) and tower shadow effect. Cut-in wind speed is 3m/s and rated wind speed is 11m/s. Fig. 9(b) shows the active power. The active power generated from induction generator shows in black line and the active power flowing to the grid shows in gray line. The generated power is depending on the wind speed. When the

equivalent wind speed is greater than cut-in wind speed (3m/s), an induction generator start to generation. When the equivalent wind speed is stronger than the rated wind speed, the output active power is limited by blade pitch control.

Fig. 10 shows the tip speed ratio and power coefficient (Cp). In Fig. 10(a), before the cut-in wind speed, the tip speed ratio increases over the optimal value but after a few seconds, controlled to be optimal value. In Fig. 10(b), the power coefficient is a function of tip speed ratio. After the cut-in wind speed, the power coefficient controlled to be maximum value.

Figs. 11(a), (b) shows the estimated d-q axes rotor flux in stationary reference frame. Figs. 11(c), (d) shows the estimated d-q axes rotor flux in synchronously rotating reference frame. In Figs. 11(c), (d), the estimated d-q axes rotor flux rapidly converge to reference value.

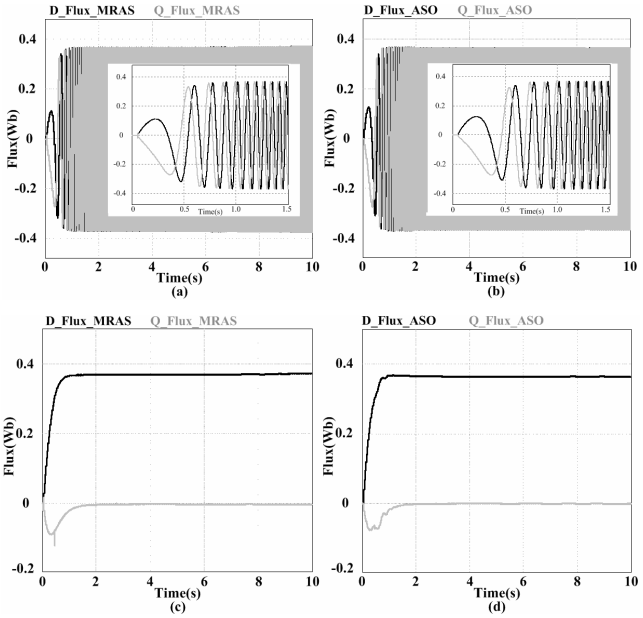

Fig. 11. Estimated d-q axes rotor flux.

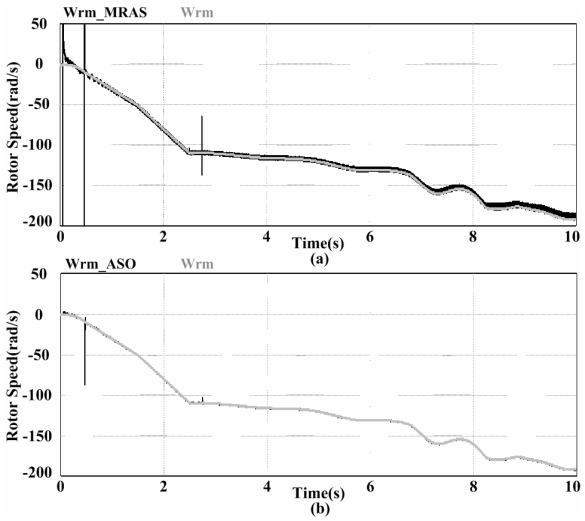

Fig. 12. Estimated and simulated rotor speed: (a) MRAS; (b) ASO

Fig. 12 shows the estimated(black) and simulated(gray) generator rotor speed. By rotor speed-torque control strategy, the rotor speed controlled from zero to rated speed. The NREL 5MW control strategy is scaled down to fit 11kW induction generator. In Fig. 12, the ASO estimation method shows better rotor speed tracking performance than the MRAS estimation method.

Fig. 13 shows the generator rotor speed error between simulated and estimated value. In Fig. 13(a), speed error of MRAS estimation method is about ± 5[rad/s] and little increase in high speed operation area. In Fig. 13(b), speed error of ASO estimation method is about ± 1[rad/s] with some peaks. In overall speed operation area, the speed tracking by ASO method shows good performance.

Fig. 14 shows the estimated(black) and simulated(gray) rotor position from $-\pi$ to π rad/s. The estimated rotor

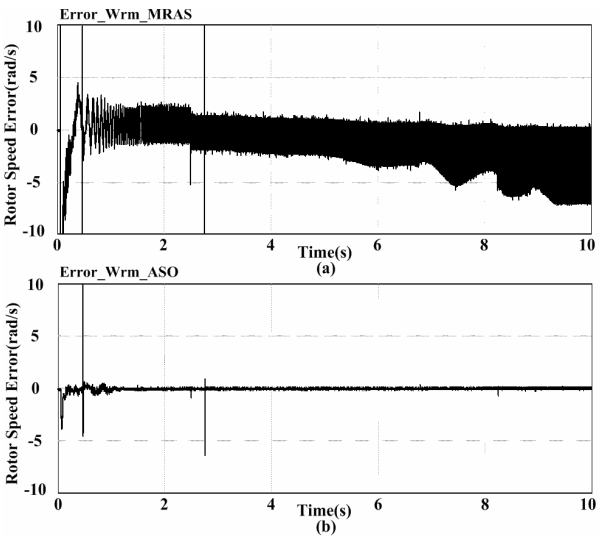

Fig. 13. Rotor speed error: (a) MRAS; (b) ASO

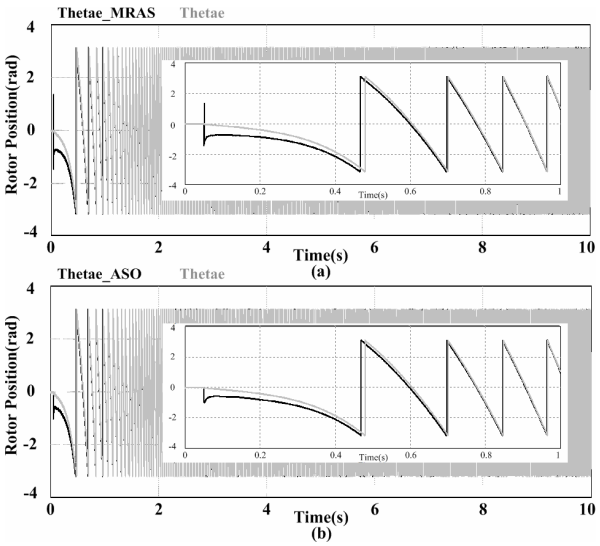

Fig. 14. Rotor position: (a) MRAS; (b) ASO

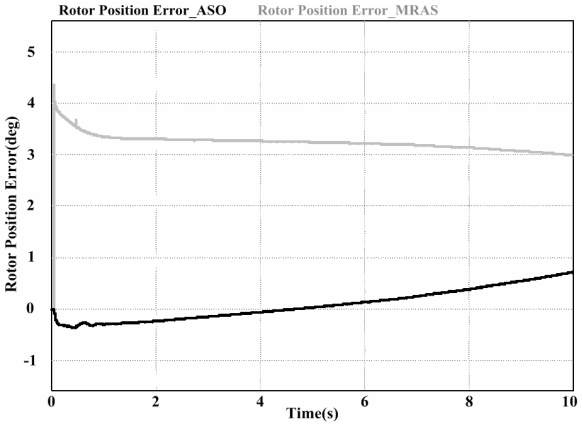

Fig. 15. Rotor position error (Gray: MRAS, black: ASO)

position very quickly follows the simulated rotor position. As shown in the Fig. 14(b), ASO estimation method shows better performance.

Fig. 15 shows the rotor position error. The position error of MRAS(gray) estimation method is about 3[deg]. The position error of ASO(black) estimation method is within ± 1[rad/s]. The position tracking by ASO method shows good performance in wide speed operation area.

6. Conclusion

In this paper, the sensorless vector control scheme of induction motors for wind energy application based on MRAS method and ASO method is described and compared. The vector control implement by using motor control inverter and back-to-back converter. Through the MRAS and ASO, the generator rotor speed and position can be estimated. Analyses and simulation results show that ASO estimation method has better performance than MRAS. The speed and position error from ASO method is about 3% and about 2% respectively. The speed and position error from MRAS method is about 5% and about 4% respectively. As a result, simulation results demonstrate the proposed sensorless algorithms fulfill the requirements of wind energy system in wide operating area

Apeendix

Parameters of 22kW induction machine:

Primary voltage 220[V], primary current 74.6[A], 22[kW], four poles, 1765 [r/min], Rs = 0.041[ohm], Ls = 13.35[mH], Rr = 0.024[ohm], Lr = 13.65[mH], Lm = 13.25 [mH]

Parameters of 11kW induction machine:

Primary voltage 180[V], primary current 45[A], 11[kW], four poles, 1750[r/min], Rs = 0.069[ohm], Ls=14.115[mH], Rr = 0.044[ohm], Lr = 14.115[mH], Lm = 13.2[mH]

References

[1] A. Miller, E. Muljadi and D. S. Zinger, "A variable speed wind turbine power control," *IEEE Trans. Energy Conversion*, vol. 12, no. 2, pp. 181-186, Jun. 1997.

[2] H. Polinder, F. F. A. van der Piji, G.-J. de Vilder and P. J. Tavner, "Comparison of direct-drive and geared generator concepts for wind turbines," *IEEE Trans. Energy Conversion*, vol. 21, no. 3, pp. 725-733, Sept. 2006.

[3] A. Consoli, S. Musumeci, A. Raciti and A. Tsesta, "Sensorelss vector control and speed control of brushless motor drives," *IEEE Trans. Ind. Electron.*, vol. 41, no. 1, pp. 91-96, Feb. 1994.

[4] T. Orlowska-Kowalska and M. Dybkowski, "Stator-Current-Based MRAS Estimator for a Wide Range Speed-Sensorless Induction-Motor Drive," *IEEE Trans. Ind. Electron.*, vol. 57, no. 4, pp. 1296-1308, Apr. 2010.

[5] Byung-Il Kwon, Hai Lin and Kyu-Yun Hwang, "An Improved Flux Observer for Sensorless Permanent Magnet Synchronous Motor Drives with Parameter Identification," *JEET*, vol. 8, no. 3, pp. 530-543, May. 2013.

[6] Kwang-Woon Lee and Jung-Ik Ha, "Evaluation of Back-EMF Estimators for Sensorless Control of Permanent Magnet Synchronous Motors," *JPE*, vol. 12, no. 4, pp. 604-614, July. 2012.

[7] M. Barut, S. Bogosyan, and M. Gokasan, "Speed-Sensorless Estimation for Induction Motors Using Extended Kalman Filters," *IEEE Trans. Ind. Electron.*, vol. 54, no. 1, pp. 272-280, Feb. 2007.

[8] M. Hajian, J. Soltani, G. A. Markadeh and S. Hosseinnia, "Adaptive Nonlinear Direct Torque Control of Sensor-less IM Drives With Efficiency Optimization," *IEEE Trans. Ind. Electron.*, vol. 57, no.3, pp. 975-985, Mar. 2010

[9] M. Pacas, "Sensorless Drives in Industrial Applications," *IEEE Ind. Electron. Magazine.* vol. 5, no. 2, pp. 16-23, June. 2011.

[10] M'hamed Sekour, Kada Hartani, Azeddine Draou and Ahmed Allali, "Sensorless Fuzzy Direct Torque Control for High Performance Electric Vehicle with Four In-Wheel Motors," *JEET*, vol. 8, no. 3, pp. 530-543, May, 2013.

[11] P. L. Jansen and R. D. Lorenz, "A physically insightful approach to the design and accuracy assessment of flux observers for field oriented induction machine drives," IEEE Trans. Ind. Appl., vol. 30, no.1, pp. 101-110, Jan/Feb, 1994.

[12] H. Kubota, K. Matsuse and T. Nakano, "DSP-Based Adaptive Flux Observer of Induction Motor," *IEEE Trans. Ind. Appl.*, Vol. 29, No.2, pp.344-348, Mar/Apr, 1993.

[13] P. Sorensen, A. D. Hansen and P. A. C. Rosas, "Wind models for simulation of power fluctuations from wind farms," *Journal of Wind Engineering and Industrial Aerodynamics.*, vol. 90, no. 12-15, pp. 1381-1402, Dec. 2002.
[14] T. Burton, D. Sharpe, N. Jenkins, and E. Bossanyi, *Wind Energy Handbook*, Wiley, 2001, p.233-235
[15] Seung-Ki Sul, *Control of Electric Machine Drive Systems*, John Wiley & Sons., 2011, p. 120-125, 243-245
[16] P. Sørensen, "Frequency domain modeling of wind turbine structures," Denmark. Forskningscenter Risoe. Risoe-R749(EN), Apr. 1994.
[17] W. Langreder, "Models for Variable Speed Wind Turbines," M.Sc. Thesis, Risø CREST Loughborough University and National Laboratory, 1996.

Il-Woo Jeong He received the B.S degree in Electrical Engineering from Soongsil University, Seoul, Korea, in 2010. Since 2011, he has been pursuing the M.S.-Ph.D. integrated course at Graduate school for Wind Energy, Pohang University of Science and Technology (POSTECH), Pohang, Korea. His research areas include are wind energy system control, motor/generator sensorless control and grid connected system control.

Won-Shik Choi He received the B.S degree in Electrical Engineering from Kyungpook National University, Daegu, Korea, in 2009, and the M.S degree in Graduate school for Wind Energy, Pohang University of Science and Technology (POSTECH), Pohang, Korea, in 2011. He is currently Ph.D. Candidate in Graduate school for Wind Energy, POSTECH, Pohang, Korea. His research areas include wind power system control, motor/generator control and power supply development.

Ki-Hyeon Park He received the Ph.D. degree in electrical engineering from Pohang University of Science and Technology (POSTECH), Pohang, Korea, in 2011. He has been a Staff Engineer in the Pohang Accelerator Laboratory (PAL) at POSTECH since 1989. His research areas include power supply development, magnetic field measurement and circuit design for ultralow signal processing.